Geophysical Research Letters

RESEARCH LETTER
10.1029/2023GL107030

The Impact of Recent Climate Change on the Global Ocean Carbon Sink

Frauke Bunsen[1], **Cara Nissen**[1,2], **and Judith Hauck**[1]

[1]Alfred Wegener Institute Helmholtz Centre for Polar and Marine Research, Bremerhaven, Germany, [2]Department of Atmospheric and Oceanic Sciences and Institute of Arctic and Alpine Research, University of Colorado, Boulder, CO, USA

Key Points:

- Climate change reduced ocean CO_2 uptake by 13% (2000–2019) primarily induced by wind-driven changes in dissolved inorganic carbon transport
- A feedback between the surface dissolved inorganic carbon concentration and air-sea flux dampens warming-driven outgassing of natural carbon
- The effect of wind changes stems primarily from high latitudes, whereas the effect of warming is globally relatively uniform

Supporting Information:

Supporting Information may be found in the online version of this article.

Correspondence to:

F. Bunsen,
frauke.bunsen@awi.de

Citation:

Bunsen, F., Nissen, C., & Hauck, J. (2024). The impact of recent climate change on the global ocean carbon sink. *Geophysical Research Letters*, *51*, e2023GL107030. https://doi.org/10.1029/2023GL107030

Received 23 NOV 2023
Accepted 15 FEB 2024

Abstract In recent decades, the ocean CO_2 uptake has increased in response to rising atmospheric CO_2. Yet, physical climate change also affects the ocean CO_2 uptake, but magnitude and driving processes are poorly understood. Using a global ocean biogeochemistry model, we find that without climate change, the mean carbon uptake 2000–2019 would have been 13% higher and the trend 1958–2019 would have been 27% higher. Changes in wind are the dominant driver of the climate effect on CO_2 uptake as they affect advective carbon transport and mixing, but the effect of warming increases over time. Roughly half of the globally integrated wind-driven trend stems from the subpolar Southern Ocean and polar oceans in both hemispheres. Warming reduces the solubility of CO_2 and acts rather homogeneously over the world oceans. However, the warming effect on pCO_2 is dampened by limited exchange of surface and deep waters.

Plain Language Summary At the ocean surface, the greenhouse gas CO_2 is exchanged between atmosphere and ocean. Because the concentration of CO_2 in the atmosphere has increased through man-made CO_2 emissions, the ocean has taken up an increasing amount of CO_2 (about 25% of the emissions). Beside the atmospheric CO_2 concentration, other climate variables affect the oceanic CO_2 uptake: Firstly, winds set the ocean in motion, drive ocean currents and thus control the transport of dissolved forms of CO_2 with ocean circulation. In particular, winds drive the exchange between the surface ocean and the deep ocean, where the bigger part of the ocean's carbon is stored. Secondly, global warming affects the oceanic CO_2 uptake because the solubility of CO_2 in water is temperature-dependent. In recent decades, changes in winds and global warming have reduced the capacity of the ocean to remove CO_2 from the atmosphere. Yet, this climate effect is not well understood. Here, we use computer simulations from 1958 to 2019 to quantify the climate effect and find that climate change reduced the oceanic CO_2 uptake of the last two decades by 13%, with winds having more of an effect than sea surface warming. The effect of warming increases over time.

1. Introduction

Besides rising atmospheric CO_2 concentrations, physical climate change also affects the oceanic CO_2 uptake (Friedlingstein et al., 2022; Sabine et al., 2004). These climate-change effects on oceanic CO_2 uptake have been a topic of intense research (Fung et al., 2005; Sarmiento et al., 1998) and it is now recognized that climate change affects the ocean carbon sink particularly through wind changes and warming (Canadell et al., 2021). Specifically, warming reduces the solubility of CO_2 in seawater and increases the stratification of the surface mixed layer, whereas changes in spatio-temporal wind patterns alter upper ocean mixing. In addition, warming and wind changes affect the large-scale overturning circulation (Canadell et al., 2021) and also affect the biological carbon pump (Henson et al., 2022).

As it is difficult to disentangle the past anthropogenic climate change signal and natural variability (McKinley et al., 2011), studies often turned to future scenarios (Fung et al., 2005; Sarmiento et al., 1998). For the recent ocean carbon sink, physical drivers have been mostly described in regional studies and from a "temporal variability" lens, often in relation to variability in climate indices, for example for the North Atlantic (Macovei et al., 2020; McKinley et al., 2011; Pérez et al., 2013) and the Southern Ocean (Hauck et al., 2013; Keppler & Landschützer, 2019; Le Quéré et al., 2007; Mayot et al., 2023). On a global scale, the climate effect was found to dampen the ocean carbon sink by around 5% (2012–2021) in a global ocean biogeochemistry model ensemble, but with no further process attribution (Friedlingstein et al., 2022). Many studies have investigated the "hiatus" in the ocean carbon sink in the 1990s, which was followed by a return to expected sink strength ("reinvigoration") since the early 2000s. The mechanisms behind this decadal variability are still unresolved (Gruber et al., 2023), with

hypotheses for the hiatus ranging from a Southern Ocean wind intensification (Le Quéré et al., 2007), through the global overturning circulation (DeVries et al., 2017) to a response to the eruption of Mount Pinatubo in conjunction with a lower atmospheric CO_2 growth rate (McKinley et al., 2020). A back-of-the-envelope calculation of the climate effect on the CO_2 flux based on CO_2 observations resulted in a rather large estimate (> 15% reduction of the net flux, Gruber et al., 2019), though this could be explained by the sensitivity of the underlying methodology to sparse data (Gloege et al., 2021; Hauck et al., 2023).

Modeling studies have the advantage of covering the whole planet and all seasons. Nevertheless, there are surprisingly few recent studies on climate drivers of the global ocean carbon sink. Doney et al. (2009) identified ocean physics as a dominant factor of interannual air-sea CO_2 flux variability, and Le Quéré et al. (2010) highlighted the dominance of winds over warming particularly for the climate-driven trend. The time period 1981–2007 investigated by Le Quéré et al. (2010) is, however, centered on the strong decadal shifts from the hiatus to the reinvigoration period. Thus, we revisit the question of the relative roles of the two dominant climate drivers, wind and warming (Canadell et al., 2021), on the long-term trend (1958–2019) and recent mean state (2000–2019) of the ocean carbon sink.

2. Methods

2.1. Ocean Biogeochemistry Model Setup and Simulations

We use the Finite Element Sea Ice-Ocean Model 1.4 (FESOM-1.4, Wang et al., 2014) coupled to the Regulated Ecosystem Model 2 (REcoM2; see Text S1 in Supporting Information S1, Hauck et al., 2013; Hauck et al., 2020; Schourup-Kristensen et al., 2014) on the CORE mesh (126,859 surface nodes; roughly equivalent to a $1° \times 1°$ resolution). Model simulations are initialized with alkalinity and preindustrial dissolved inorganic carbon (DIC) from GLODAPv2 (Lauvset et al., 2016) and nutrients from WOA2013 (Garcia et al., 2013). The model is spun up from rest for 107 years, annually repeating the atmospheric forcing for the year 1961 and using either constant (278 ppm) or increasing atmospheric CO_2 levels for the period 1850–1957 (Joos & Spahni, 2008). For the physical atmospheric forcing, we use a reanalysis product designed to drive ocean-sea-ice models (JRA55-do; Tsujino et al., 2018). Although JRA55-do is the most suitable of the available products (Tsujino et al., 2020), it must be acknowledged that, especially in the pre-satellite era, biases in the physical forcing are a significant source of inaccuracies in the modeled CO_2 flux (Le Quéré et al., 2010). The model is forced with atmospheric CO_2 from Dlugokencky and Tans (2020) as in Friedlingstein et al. (2020).

We perform six simulations (A-F, 1958–2019, Table S1 in Supporting Information S1) to disentangle the impact of climate and atmospheric CO_2 ($atmCO_2$). The total climate response is separated into the effects of wind changes, warming and a residual. Here, the effect of warming originates in the thermal surface forcing: air temperature at 10 m, specific humidity, longwave and shortwave radiation. These atmospheric forcings generate a warming signal of 0.08 °C dec^{-1} in the global mean sea surface temperature (SST) (1958–2019, Figure S1 in Supporting Information S1). Any effect of atmospheric pressure and precipitation changes on the CO_2 flux is attributed to the residual climate effect. In simulation A, climate and atmospheric CO_2 evolve from 1958 to 2019 ("historical forcing"):

$$A = \underset{\text{historical}}{atmCO_2} + \underset{\text{historical}}{climate} \quad (1)$$

In the control simulation B, the atmospheric CO_2 level is kept constant (278 ppm), and we annually repeat the year 1961 as climate forcing ("repeat-year forcing"):

$$B = \underset{\text{constant}}{atmCO_2} + \underset{\text{repeated}}{climate} \quad (2)$$

In simulations C and D, either the climate forcing (C) or atmospheric CO_2 level (D) is repeat-year or held constant, respectively:

$$C = \underset{\text{historical}}{atmCO_2} + \underset{\text{repeated}}{climate} \quad (3)$$

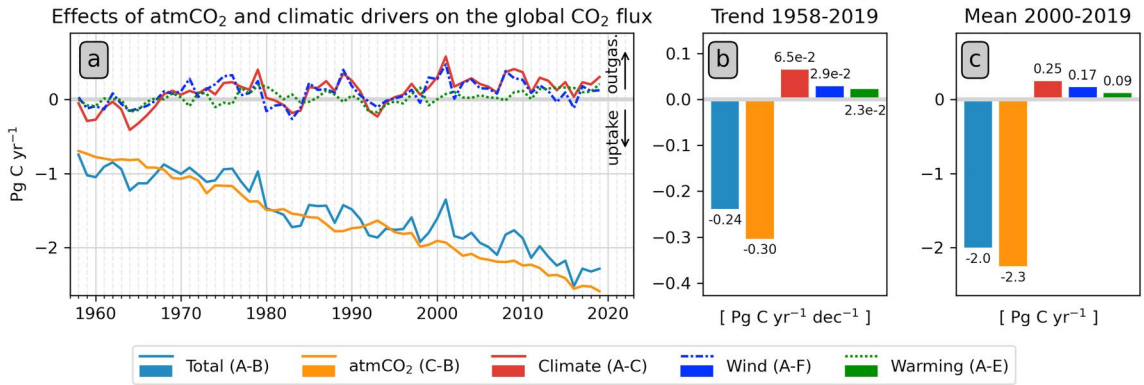

Figure 1. (a) The globally integrated CO_2 flux which arises as the sum of atmospheric CO_2 and climate effects ("total", simulation A-B) and the isolated CO_2 flux components which are driven by atmospheric CO_2 alone ("atmCO_2"), all physical drivers together ("climate"), and winds and warming separately ("wind", "warming") based on the set of simulations (b and c) The total air-sea CO_2 flux trend (1958–2019) and mean (2000–2019) and the effects of different drivers on the CO_2 flux trend and mean, respectively.

$$D = \underset{\text{constant}}{\text{atmCO}_2} + \underset{\text{historical}}{\text{climate}} \tag{4}$$

In simulation E, the atmospheric forcing is configured to remove the imprint of atmospheric warming on oceanic temperatures:

$$E = \underset{\text{historical}}{\text{atmCO}_2} + \underset{\text{repeated}}{\text{thermal}} + \underset{\text{historical}}{\text{winds}} + \underset{\text{historical}}{\text{residual climate}} \tag{5}$$

In simulation F, all forcing fields vary except for the winds:

$$F = \underset{\text{historical}}{\text{atmCO}_2} + \underset{\text{historical}}{\text{thermal}} + \underset{\text{repeated}}{\text{winds}} + \underset{\text{historical}}{\text{residual climate}} \tag{6}$$

Although the atmospheric forcing in simulations E and F is not internally consistent, the non-linearity appears to be small in the global mean as warming and wind effects add up linearly to the total climate effect (Figure 1c).

2.2. Data Analysis

We disentangle and quantify the impact of atmospheric CO_2, winds, warming and the combined climate effect firstly on the mean air-sea CO_2 flux over the two most recent decades (2000–2019) and secondly on the trend in the CO_2 flux from 1958 to 2019. In order to do this, we derive the effects of the drivers from differences between two simulations with either annually repeated forcing of the year 1961 or historically varying forcing (see Text S2 in Supporting Information S1). For example, the climate effect is quantified as simulation A minus C. Additionally, we use the different simulations to separate the climate effect on the natural CO_2 flux, that is the flux at preindustrial atmospheric CO_2; and on the anthropogenic CO_2 flux, that is the flux driven by the direct effect of increasing atmospheric CO_2 (Crisp et al., 2022; Hauck et al., 2020). By design, the primary effects of changes in the ocean's buffer factor are included in the simulations forced with increasing atmospheric CO_2.

In order to further separate the direct effect of drivers (e.g., temperature effect on CO_2 solubility) from indirect effects (e.g., circulation response), we approximate the direct effects of the following variables on the CO_2 flux analytically (Lovenduski et al., 2007): wind velocity, SST, sea-ice concentration, salinity-normalized alkalinity (sAlk), salinity and freshwater fluxes (S + FW) and salinity-normalized DIC (sDIC). Although further refinements of the method of Lovenduski et al. (2007) exist (Liao et al., 2020; Roobaert et al., 2022), we consider here this method to be sufficiently robust, capitalizing on the full representation of non-linear dependencies in the simulations (Section 2.1). Effects of changes in biological production and circulation appear in the sDIC term in this methodology. We isolate them by attributing the trend of the mixed-layer sDIC rate-of-change offline to trends in (a) biological export fluxes, (b) air-sea CO_2 fluxes or (c) circulation, advection and mixing (the latter is calculated as the residual and includes changes in the large scale overturning circulation as well as upwelling and

mixing across the base of the mixed layer; Lovenduski et al., 2007; Bunsen, 2021). An extended description of the offline attribution can be found in Text S3, Text S4 in Supporting Information S1 and Bunsen (2021).

3. Results and Discussion

3.1. Drivers of the Global CO_2 Flux

With a globally integrated oceanic CO_2 sink of -1.74 PgC yr^{-1} 1990–1999 in the bias-corrected historical simulation (A-B), FESOM1.4-REcoM2 falls within the constraints of the IPCC estimate (-2.2 ± 0.7 PgC yr^{-1}, Ciais et al., 2013). Based on the set of simulations, rising atmospheric CO_2 dominates the contemporary mean CO_2 flux (2000–2019), generating an uptake of -2.25 PgC yr^{-1} (113% of the net flux, C-B, Figures 1a and 1c). Climate change and variability reduce the mean CO_2 uptake by 0.25 PgC yr^{-1} (A-C), which is 13% of the net flux. The climate impact can be explained by the response of natural carbon (0.26 PgC yr^{-1}, D-B, Table S2 in Supporting Information S1) with little compensation by anthropogenic carbon (-0.01 PgC yr^{-1}). Of all climate forcings, wind has the largest control on the mean CO_2 flux (0.17 PgC yr^{-1} or 67% of the climate effect, Figure 1c). Its impact is largely indirect through changes in circulation and mixing, as revealed by the comparison with the offline attribution, which shows direct impacts on the gas-transfer velocity to be small (Text S5, Figure S2 and S3 in Supporting Information S1). Overall, the wind signal is larger than the contribution of global warming (0.09 PgC yr^{-1} or 35%).

Corresponding to an increase of the mean ocean uptake from -1.0 PgC yr^{-1} 1960–1979 to -2.0 PgC yr^{-1} 2000–2019, we diagnose a trend toward more uptake of -0.24 PgC yr^{-1} dec^{-1} 1958–2019 in the historical simulation (A-B). As for the mean flux, the trend is largely driven by atmospheric CO_2 (-0.30 PgC yr^{-1} dec^{-1}, 128% of the net trend, C-B, Figure 1). Despite an increase in the global mean buffer factor by approximately 20% from 1958 to 2019, we see no slow-down in the atmCO_2-driven increase of oceanic CO_2 uptake, implying that there is no detectable buffer factor effect on the global air-sea CO_2 flux in our data. However, climate change and variability reduce the 1958–2019 trend in the CO_2 uptake by 6.5×10^{-2} PgC yr^{-1} dec^{-1} (A-C), which corresponds to 27% of the net trend. Here, the wind effect marginally outweighs the effect of warming (2.9×10^{-2} PgC yr^{-1} dec^{-1} or 45% of the climate effect vs. 2.3×10^{-2} PgC yr^{-1} dec^{-1} or 35% of the climate effect).

Other ocean-only models also show a reduction of the recent mean ocean carbon sink through climate change (4.3%–10.3% of the net flux, 2013–2022, Friedlingstein et al., 2023, see also DeVries et al., 2023). The temporal evolution of FESOM1.4-REcoM2 and the models in Friedlingstein et al. (2023) is in qualitative agreement with atmospheric inversions that ingest atmospheric CO_2 observations from around the world. Multiple lines of observation-based evidence support climate-change effects on the ocean carbon sink (Keppler et al., 2023; Mignot et al., 2022; Müller et al., 2023) in addition to theoretical understanding (Canadell et al., 2021), but we acknowledge that studies based on ocean observations are sensitive to sparse sampling (Gloege et al., 2021; Hauck et al., 2023) and interannual and decadal variability (Ballantyne et al., 2012). Indeed, interannual variability masks any continuous trend of the ocean-borne fraction of global CO_2 emissions attributable to climate change in the historical simulation of FESOM1.4-REcoM2. Nevertheless, our set of simulations demonstrates that the historical ocean-borne fraction is below the value it would have had without climate change and variability since 1985 (Figure S4 in Supporting Information S1). As our model simulations cover the period 1958–2019, the impact of interannual and decadal variability on the reported long-term climate-change trends is likely small, whereas shorter periods are sensitive to temporal variability and thus also to chosen start and end years. We also note the simulated increase in the relative importance of warming over time in our model simulations. Looking at different time periods for the mean flux, the contribution of warming has recently increased from about 10% of the climate effect (1981–2007, 1994–2007) to 35% (2000–2019, Table S2 in Supporting Information S1). Yet, as wind dominates the mean flux relative to warming for all assessed time windows, this finding is in agreement with Le Quéré et al. (2010).

Interestingly, the warming-driven CO_2 flux trend based on the set of simulations is substantially smaller than the linear offline approximation of the temperature effect (0.19 PgC yr^{-1} dec^{-1}; Text S6 and Figure S3 in Supporting Information S1), which we attribute to a negative feedback involving sDIC (Figure 2a). The solubility effect of warming captured by the offline approximation is an outgassing of natural CO_2 at the surface. However, the set of simulations additionally accounts for the decrease in the surface concentration of natural sDIC as a result of outgassing. This decrease, in turn, attenuates the outgassing. The strength of this dampening feedback depends on how fast surface waters warmed by climate change and with low natural sDIC are replaced by waters from below

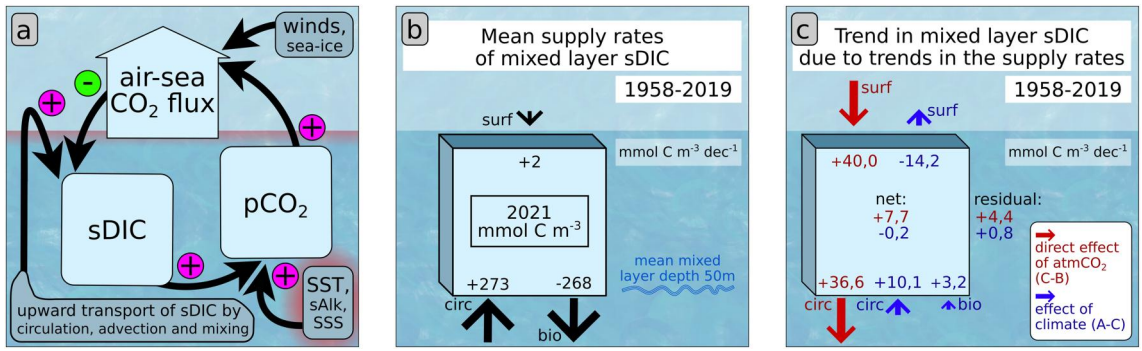

Figure 2. (a) A negative feedback between the air-sea CO_2 flux and the mixed layer salinity-normalized dissolved inorganic carbon (sDIC) concentration dampens the warming-driven outgassing of natural CO_2. However, this feedback is weakened through net-upward transport of natural sDIC through circulation, advection and mixing. (b) The mean mixed layer sDIC concentration 1958–2019 in the historical simulation A and the mean supply rates of sDIC through the air-sea CO_2 flux (J_{surf}), export production (J_{bio}) and circulation, advection and mixing (J_{circ}); all are calculated at the local mixed-layer depth and then averaged globally. (c) The trend in mixed layer sDIC concentration 1958–2019 due to trends in J_{surf}, J_{circ} and J_{bio} separated into CO_2 and climate effects.

through upwelling and mixing, which have not yet been affected as much by warming. The more water is transported to the surface and subsequently warms, the less important is the feedback and the stronger is the thermally driven outgassing (see e.g. equatorial regions in Figure 3f).

Compared over the same time periods, the response of the CO_2 flux to climate-change in FESOM1.4-REcoM2 is in line with recent model estimates (Friedlingstein et al., 2023), but is smaller than the previous estimates of the mean or trend by Le Quéré et al. (2010) and Gruber et al. (2019) (see Table S2 in Supporting Information S1). Specifically, both the effect of rising atmospheric CO_2 and the back-of-the-envelope climate-effect on natural carbon are larger in the observation-based estimate of Gruber et al. (2019). The FESOM1.4-REcoM2 estimates are also lower than the CO_2-, warming- and wind-effects in Le Quéré et al. (2010). The smaller air-sea flux driven by atmospheric CO_2 in FESOM1.4-REcoM2 suggests that the removal of anthropogenic sDIC from the mixed layer into the intermediate and deep ocean through advection and mixing is less efficient (DeVries et al., 2017; Goris et al., 2018), while the smaller effect of warming on the CO_2 flux in FESOM1.4-REcoM2 suggests that the upward transport of cool waters with potential for thermal outgassing is smaller. All in all, the transport of sDIC in FESOM1.4-REcoM2 is slower. Differences in the model physics are known to give rise to considerable inter-model spread in the biogeochemical fields (Doney et al., 2004; Terhaar et al., 2023) as the strength of over-turning varies by 20%–30% between models (Huber & Zanna, 2017). With a maximum streamfunction of 12.2 Sv at 26N, the Atlantic Meridional Overturning Circulation in our historical simulation falls within the lower range of other ocean circulation models and observations (11–19 Sv, Hirschi et al., 2020), which is an indication for less sDIC transport and thus supports our interpretation.

3.2. Attribution of Global Trends in sDIC to the Variability in Air-Sea CO_2 flux, Biology and Circulation

As demonstrated by the air-sea CO_2 flux-sDIC feedback (Figure 2a), changes in the air-sea carbon exchange can be cause and result of variability in mixed-layer sDIC. Circulation, advection and mixing as well as biology are also part of this interplay. On a global scale, the sinking of particulate organic carbon through the base of the mixed layer (J_{bio}) constitutes a sink for mixed layer sDIC in the long-term (1958–2019; Figure 2b). The net supply of sDIC through vertical advection and mixing (J_{circ}) constitutes a source for the mixed layer and is of the same order of magnitude as J_{bio}, illustrating that (a) upwelling of sDIC-rich deep waters outweighs the downward transport of low-DIC waters, and (b) that J_{bio} and J_{circ} nearly balance. The air-sea CO_2 flux works to reduce the small imbalance between J_{bio} and J_{circ}. Thus, even small changes of the supply rates can lead to an impactful trend in the surface CO_2 flux.

As expected from the analysis in Section 3.1, the net trend in the global mean mixed-layer sDIC concentration is positive, largely due to the increasing atmospheric CO_2 (Figure 2c). In fact, the mixed-layer sDIC would increase much faster without the compensating effect toward enhanced downward transport of anthropogenic sDIC (by 40.0 mmolC m^{-3} dec^{-1} instead of 7.7 mmolC m^{-3} dec^{-1}). Even though much smaller in magnitude, the reduced solubility of CO_2 in the mixed layer due to global warming drives a negative component in the trend

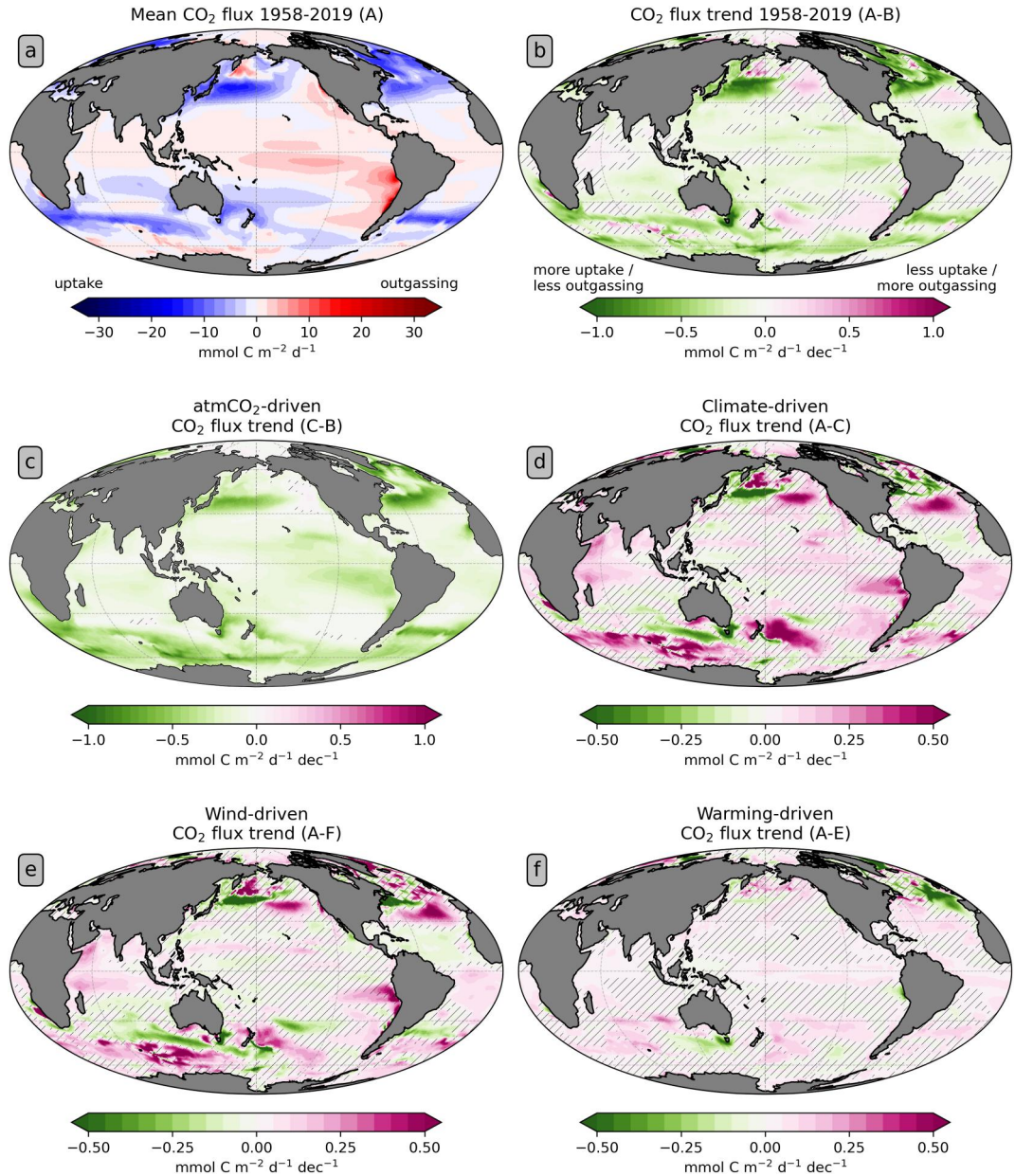

Figure 3. (a) The mean air-sea CO_2 flux density and (b) trend in the CO_2 flux density 1958–2019 in the historical simulation (simulation A) (c–f) The effects of the rising atmospheric CO_2 concentration and climate change on the trend in the CO_2 flux density obtained as the difference between two simulations with and without interannual variability and trends in the respective variable(s): (c) Atmospheric CO_2 concentration, (d) full climate variability and trends, (e) winds and (f) global warming. Positive values denote a trend toward more oceanic outgassing or less oceanic uptake, respectively. Hatched areas in (b–f) indicate a low significance of the trend (p-value > 0.05 applying a two-sided Wald Test with t-distribution).

(-0.7 mmolC m^{-3} dec^{-1}; not shown). This component is dampened by the wind signal and wind- and warming-driven interactions to result in a climate-driven negative sDIC signal of -0.2 mmolC m^{-3} dec^{-1}.

With the mixed-layer budget, we can demonstrate that climate change leads to higher sDIC input to the mixed-layer. This is due to wind-driven changes in circulation and mixing and through reduced biological carbon export, although the biological signal is smaller than the physical one (Figure 2c). The higher sDIC input and the warming of the surface ocean then trigger the climate-induced loss of CO_2 to the atmosphere and the negative feedback that was identified in section Section 3.1 (see also Figure 2a). Overall, this analysis demonstrates how the interplay of

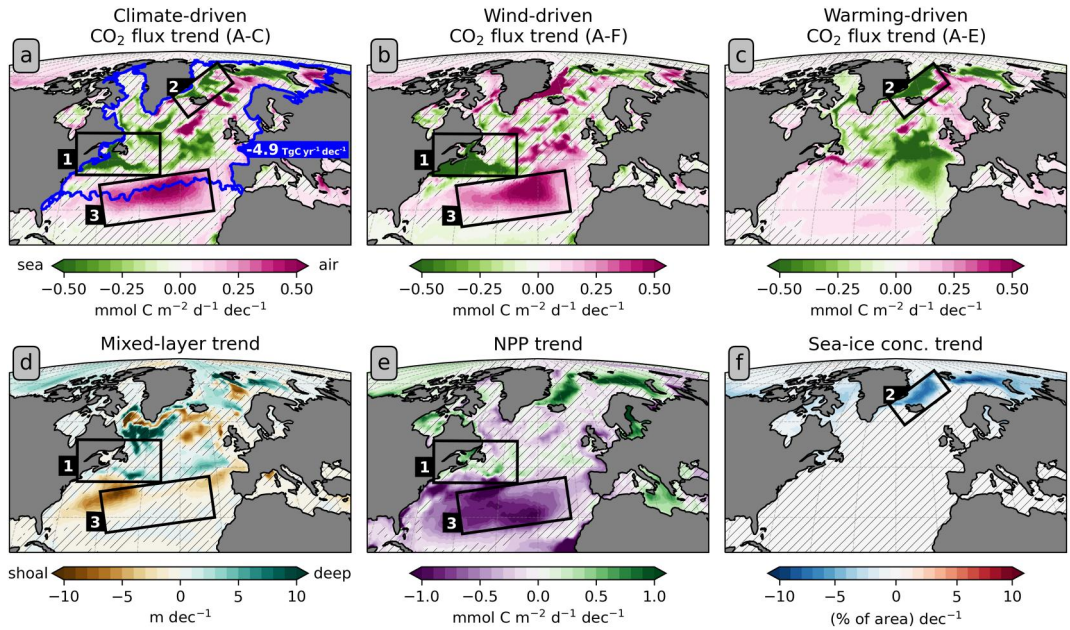

Figure 4. (a–c) Trends in the CO_2 flux density between 1958 and 2019 due to (a) net climate effects, (b) winds and (c) global warming (d–f) Trends in (d) mixed layer depth, (e) net primary productivity and (f) sea-ice concentration. Hatched areas indicate a low significance of the trend (p-values > 0.05). The blue framed area indicates the North Atlantic biomes defined by Fay and McKinley (2014) (Figure S6 in Supporting Information S1).

changes in atmospheric CO_2, ocean circulation, mixing and surface warming shapes the air-sea flux trend, while the role of biological processes is minor (see also Lovenduski et al., 2007).

3.3. Regional Processes

Regionally, the relative role of different drivers in controlling CO_2 flux trends varies. Particularly strong trends in the CO_2 flux density toward more uptake driven by the increase in atmospheric CO_2 are found in the high-uptake regions (northern North Atlantic and approx. 30–40°N/S, Figures 3a–3c). In addition, strong trends toward less outgassing occur in the Southern Ocean around 60°S. Spatial patterns of climate-change effects on the mean and trend are largely consistent (Figure 3 and Figure S5 in Supporting Information S1). The warming-driven trend in the CO_2 flux density is rather uniform globally (Figure 3f), with the large subtropical and tropical oceans dominating the globally integrated flux trend (Figure S6 in Supporting Information S1). In contrast, the wind-driven trend in the CO_2 flux density is more heterogeneous (Figure 3e), with roughly half of the globally integrated flux trend stemming from the subpolar Southern Ocean and polar oceans in both hemispheres (Figure S6 in Supporting Information S1). As a result, the global climate effect results from a mosaic of different regional and interacting processes.

The northern North Atlantic is exposed to regional climate change that, collectively, promotes greater oceanic CO_2 uptake (-4.9 TgC yr^{-1} dec^{-1}, Figure 4). The reasons are twofold: firstly, the intensification of westerly winds, mixed layer deepening and increasing net primary productivity (NPP) in the western North Atlantic lead to more CO_2 uptake (Figure 4, region 1). Secondly, the retreat of sea-ice due to warming drives increased CO_2 uptake and increased NPP east of Greenland (Figure 4, region 2). For this region, our offline approximation confirms that the retreat of Arctic sea-ice is by far the most important climate driver of the increase in CO_2 uptake (offline analysis not shown, Yasunaka et al., 2023). Additionally, there is observational evidence for the loss of sea-ice (Meredith et al., 2019) driving increased NPP (Kahru et al., 2016). In contrast, in the subtropical North Atlantic, weaker winds and a more negative wind stress curl constitute more favorable conditions for subduction and lead to less CO_2 uptake, which is driven by decreased NPP and export production in that area (Figure 4, region 3). While a decrease in NPP has been observed, it was attributed to warming (Siemer et al., 2021). Climate-driven changes of the North Pacific CO_2 flux exhibit similar features and we attribute them to similar changes in winds (Text S7 and Figure S7 in Supporting Information S1).

In the subtropics and tropics, climate change leads to greater outgassing of CO_2 in total (45 TgC yr^{-1} dec^{-1}, Figure S8 in Supporting Information S1). Both warming and winds play equally important roles in driving this effect. Among others, there are extensive areas in the northern Indian Ocean where increased outgassing is found due to a combination of warming, weakening winds, and a shallower mixed layer. In particular in the Arabian Sea, the primary driver of increased outgassing is a decrease in biological productivity caused by stronger stratification and warming, which is also evident from observations (Dalpadado et al., 2021; Roxy et al., 2016). Furthermore, an intensification of upwelling-favorable winds, as observed by Sydeman et al. (2014) and Varela et al. (2015), drives increased outgassing in the California, Humboldt, Benguela and south-west Australian Boundary Upwelling Systems.

In the Southern Ocean, the net effect of climate is to promote increased outgassing of CO_2 (25 TgC yr^{-1} dec^{-1}, Figure S9 in Supporting Information S1), and this effect is dominated by changes in winds. Specifically, the strengthening of westerly winds leads to more upwelling of natural carbon and subsequent outgassing of CO_2 (Hauck et al., 2013; Le Quéré et al., 2007; Lovenduski et al., 2007). In the Indian sector, both positive and negative effects of climate change exist, with more upwelling of DIC in the Antarctic ocean and at the Polar Front complemented by more subduction equatorward (Panassa, 2018). This, in combination with a deepening of the mixed layer and an increase in NPP in the sub-Antarctic, promotes a greater uptake of CO_2 locally.

4. Conclusion

It is unambiguous that the ocean carbon sink has increased over recent decades in line with increasing atmospheric CO_2 levels as its primary driver (Ballantyne et al., 2012; DeVries et al., 2023; Gruber et al., 2023; Müller et al., 2023). However, our model simulations show that the trend of the global CO_2 flux 1958–2019 would be 27% (6.5×10^{-2} PgC yr^{-1} dec^{-1}) higher without climate change and variability; and correspondingly, the mean flux 2000–2019 would be 13% higher (0.25 PgC yr^{-1}, Figure 1). Wind-driven changes in mixing and advective transport of sDIC lead to less CO_2 uptake and constitute the most important climatic driver globally. Warming is the second most important driver of climate-induced changes in ocean carbon uptake. Warming-induced changes of the CO_2 flux are regulated through a feedback between warming, air-sea CO_2 flux, surface sDIC concentration and vertical sDIC transport. In FESOM1.4-REcoM, the climate-related outgassing of natural CO_2 is weaker than in previous studies, calling for a dedicated multi-model analysis on the climate-change effects on the ocean CO_2 uptake. If anthropogenic CO_2 emissions abate in the future, the anthropogenic component of the air-sea CO_2 flux directed into the ocean is expected to stop growing. In contrast, the trend in the air-sea CO_2 flux toward more outgassing of natural CO_2 driven by climate change is expected to persist longer (Solomon et al., 2009). Therefore, understanding and realistically simulating the CO_2-driven and climate-driven components of the CO_2 flux is highly relevant for projections of the atmospheric CO_2 evolution.

Data Availability Statement

The data used in this manuscript was created with the General Ocean Circulation and Sea-Ice Model FESOM1.4 (Wang et al., 2014) coupled to the biogeochemistry model REcoM2 (Schourup-Kristensen et al., 2014), using ESM tools (Barbi et al., 2021). FESOM and REcoM continue to be further developed and are publicly available under a GNU GPL licence. The source code version and set-up used for this study can be found at: 10.5281/zenodo.10201713. Processed model output underlying the figures of this manuscript is available at: 10.5281/zenodo.6908190. We used pyfesom (Koldunov et al., 2016) to work with model output on the unstructured mesh. For the offline analysis of model data, we used xarray v0.16.2 (Hoyer et al., 2020; Hoyer & Hamman, 2017), pandas v1.2.0 (McKinney, 2010; Reback et al., 2020), scipy 1.6.0 (Virtanen, Gommers, Burovski, et al., 2020; Virtanen, Gommers, Oliphant, et al., 2020) and python-seawater (Fernandes, 2014). Figures were created with matplotlib v3.3.3 (Caswell et al., 2020; Hunter, 2007) and cartopy v0.15.0 (Met Office, 2015).

Acknowledgments
This research has received funding from the Helmholtz Young Investigator Group Marine Carbon and Ecosystem Feedbacks in the Earth System (MarESys, Grant VH-NG-1301), from the European Union's Horizon 2020 Research and Innovation Programme under Grant 820989 (COMFORT) and from the European Research Council Starting Grant ERC-2022-STG OceanPeak (Grant 101077209). The work reflects only the authors' view; the European Commission and their executive agency are not responsible for any use that may be made of the information the work contains. Open Access funding enabled and organized by Projekt DEAL.

References

Ballantyne, A., Alden, C., Miller, J., Tans, P., & White, J. (2012). Increase in observed net carbon dioxide uptake by land and oceans during the past 50 years. *Nature*, *488*(7409), 70–72. https://doi.org/10.1038/nature11299

Barbi, D., Wieters, N., Gierz, P., Andrés-Martínez, M., Ural, D., Chegini, F., et al. (2021). ESM-tools version 5.0: A modular infrastructure for stand-alone and coupled earth system modelling (ESM). *Geoscientific Model Development*, *14*(6), 4051–4067. https://doi.org/10.5194/gmd-14-4051-2021

Bunsen, F. (2021). *Impact of recent climate variability on oceanic CO_2 uptake in a global ocean biogeochemistry model*. Master Thesis. Kiel University Christian-Albrechts-Universität. https://doi.org/10.3289/MSC_2021_Bunsen

Canadell, J., Monteiro, P., Costa, M., Cotrim da Cunha, L., Cox, P., Eliseev, A., et al. (2021). Global carbon and other biogeochemical cycles and feedbacks, (Eds.). In *Climate change 2021: The physical science basis. Contribution of working Group I to the sixth assessment report of the intergovernmental panel on climate change* (pp. 673–816). Cambridge University Press. https://doi.org/10.1017/9781009157896.007

Caswell, T. A., Droettboom, M., Lee, A., Hunter, J., de Andrade, E. S., Firing, E., et al. (2020). matplotlib/matplotlib: Rel: v3.3.3 [Software]. *Zenodo*. https://doi.org/10.5281/zenodo.4268928

Ciais, P., Sabine, C., Bala, G., Bopp, L., Brovkin, V., Canadell, J. G., et al. (2013). Carbon and other biogeochemical cycles, (Eds.). In *Climate change 2013: The physical science basis. Contribution of working Group I to the fifth assessment report of the intergovernmental panel on climate change* (pp. 465–570). Cambridge University Press. https://doi.org/10.1017/CBO9781107415324.015

Crisp, D., Dolman, H., Tanhua, T., McKinley, G. A., Hauck, J., Bastos, A., et al. (2022). How well do we understand the land-ocean-atmosphere carbon cycle? *Reviews of Geophysics*, *60*(2), e2021RG000736. https://doi.org/10.1029/2021RG000736

Dalpadado, P., Arrigo, K. R., van Dijken, G. L., Gunasekara, S. S., Ostrowski, M., Bianchi, G., & Sperfeld, E. (2021). Warming of the Indian Ocean and its impact on temporal and spatial dynamics of primary production. *Progress in Oceanography*, *198*, 102688. https://doi.org/10.1016/j.pocean.2021.102688

De Vries, T., Holzer, M., & Primeau, F. (2017). Recent increase in oceanic carbon uptake driven by weaker upper-ocean overturning. *Nature*, *542*(7640), 215–218. https://doi.org/10.1038/nature21068

DeVries, T., Yamamoto, K., Wanninkhof, R., Gruber, N., Hauck, J., Müller, J. D., et al. (2023). Magnitude, trends, and variability of the global ocean carbon sink from 1985 to 2018. *Global Biogeochemical Cycles*, *37*(10), e2023GB007780. https://doi.org/10.1029/2023GB007780

Dlugokencky, E., & Tans, P. (2020). Trends in atmospheric carbon dioxide [Dataset]. National Oceanic and Atmospheric Administration, Earth System Research Laboratory (NOAA/ESRL). Retrieved from http://www.esrl.noaa.gov/gmd/ccgg/trends/global.html

Doney, S. C., Lima, I., Feely, R. A., Glover, D. M., Lindsay, K., Mahowald, N., et al. (2009). Mechanisms governing interannual variability in upper-ocean inorganic carbon system and air–sea CO_2 fluxes: Physical climate and atmospheric dust. *Deep Sea Research Part II: Topical Studies in Oceanography*, *56*(8), 640–655. https://doi.org/10.1016/j.dsr2.2008.12.006

Doney, S. C., Lindsay, K., Caldeira, K., Campin, J.-M., Drange, H., Dutay, J.-C., et al. (2004). Evaluating global ocean carbon models: The importance of realistic physics. *Global Biogeochemical Cycles*, *18*(3), GB3017. https://doi.org/10.1029/2003GB002150

Fay, A. R., & McKinley, G. A. (2014). Global open-ocean biomes: Mean and temporal variability. *Earth System Science Data*, *6*(2), 273–284. https://doi.org/10.5194/essd-6-273-2014

Fernandes, F. (2014). Python-seawater [Software]. *Zenodo*. https://doi.org/10.5281/zenodo.11395

Friedlingstein, P., Jones, M. W., O'Sullivan, M., Andrew, R. M., Bakker, D. C. E., Hauck, J., et al. (2022). Global carbon budget 2021. *Earth System Science Data*, *14*(4), 1917–2005. https://doi.org/10.5194/essd-14-1917-2022

Friedlingstein, P., O'Sullivan, M., Jones, M. W., Andrew, R. M., Bakker, D. C. E., Hauck, J., et al. (2023). Global carbon budget 2023. *Earth System Science Data*, *15*(12), 5301–5369. https://doi.org/10.5194/essd-15-5301-2023

Friedlingstein, P., O'Sullivan, M., Jones, M. W., Andrew, R. M., Hauck, J., Olsen, A., et al. (2020). Global carbon budget 2020. *Earth System Science Data*, *12*(4), 3269–3340. https://doi.org/10.5194/essd-12-3269-2020

Fung, I. Y., Doney, S. C., Lindsay, K., & John, J. (2005). Evolution of carbon sinks in a changing climate. *Proceedings of the National Academy of Sciences*, *102*(32), 11201–11206. https://doi.org/10.1073/pnas.0504949102

Garcia, H. E., Locarnini, R. A., Boyer, T. P., Antonov, J. I., Baranova, O. K., Zweng, M. M., et al. (2013). World Ocean Atlas. *Dissolved inorganic nutrients (Phosphate, Nitrate, Silicate)* (Vol. 4). U.S. Department of Commerce, National Oceanic and Atmospheric Administration, National Environmental Satellite, Data and Information Service. https://doi.org/10.7289/V5J67DWD

Gloege, L., McKinley, G. A., Landschützer, P., Fay, A. R., Frölicher, T. L., Fyfe, J. C., et al. (2021). Quantifying errors in observationally based estimates of ocean carbon sink variability. *Global Biogeochemical Cycles*, *35*(4), e2020GB006788. https://doi.org/10.1029/2020GB006788

Goris, N., Tjiputra, J. F., Olsen, A., Schwinger, J., Lauvset, S. K., & Jeansson, E. (2018). Constraining projection-based estimates of the future North Atlantic carbon uptake. *Journal of Climate*, *31*(10), 3959–3978. https://doi.org/10.1175/JCLI-D-17-0564.1

Gruber, N., Bakker, D., DeVries, T., Gregor, L., Hauck, J., Landschützer, P., et al. (2023). Trends and variability in the ocean carbon sink. *Nature Reviews Earth and Environment*, *4*(2), 119–134. https://doi.org/10.1038/s43017-022-00381-x

Gruber, N., Clement, D., Carter, B. R., Feely, R. A., van Heuven, S., Hoppema, M., et al. (2019). The oceanic sink for anthropogenic CO_2 from 1994 to 2007. *Science*, *363*(6432), 1193–1199. https://doi.org/10.1126/science.aau5153

Hauck, J., Nissen, C., Landschützer, P., Rödenbeck, C., Bushinsky, S., & Olsen, A. (2023). Sparse observations induce large biases in estimates of the global ocean CO_2 sink: An Ocean Model subsampling experiment. *Philosophical Transactions of the Royal Society A: Mathematical, Physical & Engineering Sciences*, *381*(2249), 20220063. https://doi.org/10.1098/rsta.2022.0063

Hauck, J., Völker, C., Wang, T., Hoppema, M., Losch, M., & Wolf-Gladrow, D. A. (2013). Seasonally different carbon flux changes in the southern ocean in response to the southern annular mode. *Global Biogeochemical Cycles*, *27*(4), 1236–1245. https://doi.org/10.1002/2013GB004600

Hauck, J., Zeising, M., Le Quéré, C., Gruber, N., Bakker, D. C. E., Bopp, L., et al. (2020). Consistency and challenges in the ocean carbon sink estimate for the global carbon budget. *Frontiers in Marine Science*, *7*, 571720. https://doi.org/10.3389/fmars.2020.571720

Henson, S. A., Laufkötter, C., Leung, S., Giering, S., Palevsky, H., & Cavan, E. (2022). Uncertain response of ocean biological carbon export in a changing world. *Nature Geoscience*, *15*(4), 248–254. https://doi.org/10.1038/s41561-022-00927-0

Hirschi, J. J.-M., Barnier, B., Böning, C., Biastoch, A., Blaker, A. T., Coward, A., et al. (2020). The Atlantic meridional overturning circulation in high-resolution models. *Journal of Geophysical Research: Oceans*, *125*(4). https://doi.org/10.1029/2019JC015522

Hoyer, S., & Hamman, J. (2017). xarray: N-D labeled arrays and datasets in Python. *Journal of Open Research Software*, *5*(1), 10. https://doi.org/10.5334/jors.148

Hoyer, S., Hamman, J., Roos, M., Cherian, D., Fitzgerald, C., Fujii, K., et al. (2020). pydata/xarray: v0.16.2 [Software]. *Zenodo*. https://doi.org/10.5281/zenodo.4299126

Huber, M. B., & Zanna, L. (2017). Drivers of uncertainty in simulated Ocean Circulation and heat uptake. *Geophysical Research Letters*, *44*(3), 1402–1413. https://doi.org/10.1002/2016GL071587

Hunter, J. D. (2007). Matplotlib: A 2D graphics environment. *Computing in Science and Engineering*, *9*(03), 90–95. https://doi.org/10.1109/MCSE.2007.55

Joos, F., & Spahni, R. (2008). Rates of change in natural and anthropogenic radiative forcing over the past 20,000 years. *Proceedings of the National Academy of Sciences*, *105*(5), 1425–1430. https://doi.org/10.1073/pnas.0707386105

Kahru, M., Lee, Z., Mitchell, B. G., & Nevison, C. D. (2016). Effects of sea ice cover on satellite-detected primary production in the Arctic Ocean. *Biology Letters*, *12*(2), 20160223. https://doi.org/10.1098/rsbl.2016.0223

Keppler, L., & Landschützer, P. (2019). Regional wind variability modulates the southern ocean carbon sink. *Scientific Reports*, *9*(1), 7384. https://doi.org/10.1038/s41598-019-43826-y

Keppler, L., Landschützer, P., Lauvset, S. K., & Gruber, N. (2023). Recent trends and variability in the oceanic storage of dissolved inorganic carbon. *Global Biogeochemical Cycles*, *37*(5), e2022GB007677. https://doi.org/10.1029/2022GB007677

Koldunov, N., Rackow, T., Gierz, P., Rietbroek, R., Sidorenko, D., & Streffing, J. (2016). Fesom/pyfesom [Software]. Retrieved from https://pyfesom.readthedocs.io/en/latest/index.html

Lauvset, S. K., Key, R. M., Olsen, A., van Heuven, S., Velo, A., Lin, X., et al. (2016). A new global interior ocean mapped climatology: The 1°×1° GLODAP version 2 [Dataset]. *Earth System Science Data*, *8*(2), 325–340. https://doi.org/10.5194/essd-8-325-2016

Le Quéré, C., Rödenbeck, C., Buitenhuis, E. T., Conway, T. J., Langenfelds, R., Gomez, A., et al. (2007). Saturation of the southern ocean CO_2 sink due to recent climate change. *Science*, *316*(5832), 1735–1738. https://doi.org/10.1126/science.1136188

Le Quéré, C., Takahashi, T., Buitenhuis, E. T., Rödenbeck, C., & Sutherland, S. C. (2010). Impact of climate change and variability on the global oceanic sink of CO_2. *Global Biogeochemical Cycles*, *24*(4), e2020GB006574. https://doi.org/10.1029/2009GB003599

Liao, E., Resplandy, L., Liu, J., & Bowman, K. W. (2020). Amplification of the ocean carbon sink during El Niños: Role of poleward Ekman transport and influence on atmospheric CO2. *Global Biogeochemical Cycles*, *34*(9), GB6574. https://doi.org/10.1029/2020GB006574

Lovenduski, N. S., Gruber, N., Doney, S. C., & Lima, I. D. (2007). Enhanced CO_2 outgassing in the Southern Ocean from a positive phase of the southern annular mode. *Global Biogeochemical Cycles*, *21*(2), GB2026. https://doi.org/10.1029/2006GB002900

Macovei, V. A., Hartman, S. E., Schuster, U., Torres-Valdés, S., Moore, C. M., & Sanders, R. J. (2020). Impact of physical and biological processes on temporal variations of the ocean carbon sink in the mid-latitude North Atlantic (2002–2016). *Progress in Oceanography*, *180*, 102223. https://doi.org/10.1016/j.pocean.2019.102223

Mayot, N., Le Quéré, C., Rödenbeck, C., Bernardello, R., Bopp, L., Djeutchouang, L. M., et al. (2023). Climate-driven variability of the southern ocean CO_2 sink. *Philosophical Transactions of the Royal Society A: Mathematical, Physical & Engineering Sciences*, *381*(2249), 20220055. https://doi.org/10.1098/rsta.2022.0055

McKinley, G., Fay, A., Takahashi, T., & Metzl, N. (2011). Convergence of atmospheric and North Atlantic carbon dioxide trends on multidecadal timescales. *Nature Geoscience*, *4*(9), 606–610. https://doi.org/10.1038/ngeo1193

McKinley, G., Fay, A. R., Eddebbar, Y. A., Gloege, L., & Lovenduski, N. S. (2020). External forcing explains recent decadal variability of the ocean carbon sink. *AGU Advances*, *1*(2), e2019AV000149. https://doi.org/10.1029/2019AV000149

McKinney, W. (2010). Data structures for statistical computing in Python. In S. van der Walt & J. Millman (Eds.), *Proceedings of the 9th Python in science conference* (pp. 56–61). https://doi.org/10.25080/Majora-92bf1922-00a

Meredith, M., Sommerkorn, M., Cassotta, S., Derksen, C., Ekaykin, A., Hollowed, A., et al. (2019). Polar regions. In H.-O. Pörtner (Ed.), *IPCC special report on the Ocean and cryosphere in a changing climate* (pp. 203–320). Cambridge University Press. https://doi.org/10.1017/9781009157964.005

Met Office. (2015). Cartopy: A cartographic python library with a matplotlib interface. Retrieved from http://scitools.org.uk/cartopy

Mignot, A., von Schuckmann, K., Landschützer, P., Gasparin, F., & van Gennip, S. (2022). Decrease in air-sea CO_2 fluxes caused by persistent marine heatwaves. *Nature Communications*, *13*(1), 4300. https://doi.org/10.1038/s41467-022-08611-3

Müller, J. D., Gruber, N., Carter, B., Feely, R., Ishii, M., Lange, N., et al. (2023). Decadal trends in the oceanic storage of anthropogenic carbon from 1994 to 2014. *AGU Advances*, *4*, e2023AV000875. https://doi.org/10.1029/2023AV000875

Panassa, E. (2018). Role of mixed layer depth and subduction processes for the Southern Ocean carbon and nutrient cycles. PhD Thesis. *Universität Bremen*. Retrieved from https://media.suub.uni-bremen.de/handle/elib/1427

Pérez, F., Mercier, H., Vázquez-Rodríguez, M., Lherminier, P., Velo, A., Pardo, P., et al. (2013). Atlantic Ocean CO_2 uptake reduced by weakening of the meridional overturning circulation. *Nature Geoscience*, *6*(2), 146–152. https://doi.org/10.1038/ngeo1680

Reback, J., McKinney, W., vanden Bossche, J., Augspurger, T., Cloud, P., Klein, A., et al. (2020). pandas-dev/pandas: Pandas 1.2.0 [Software]. *Zenodo.* https://doi.org/10.5281/zenodo.4394318

Roobaert, A., Resplandy, L., Laruelle, G. G., Liao, E., & Regnier, P. (2022). A framework to evaluate and elucidate the driving mechanisms of coastal sea surface pCO_2 seasonality using an ocean general circulation model (MOM6-COBALT). *Ocean Science*, *18*(1), 67–88. https://doi.org/10.5194/os-18-67-2022

Roxy, M. K., Modi, A., Murtugudde, R., Valsala, V., Panickal, S., Prasanna Kumar, S., et al. (2016). A reduction in marine primary productivity driven by rapid warming over the tropical Indian Ocean. *Geophysical Research Letters*, *43*(2), 826–833. https://doi.org/10.1002/2015GL066979

Sabine, C. L., Feely, R. A., Gruber, N., Key, R. M., Lee, K., Bullister, J. L., et al. (2004). The oceanic sink for anthropogenic CO_2. *Science*, *305*(5682), 367–371. https://doi.org/10.1126/science.1097403

Sarmiento, J. L., Hughes, T., Stouffer, R., & Manabe, S. (1998). Simulated response of the ocean carbon cycle to anthropogenic climate warming. *Nature*, *393*(6682), 245–249. https://doi.org/10.1038/30455

Schourup-Kristensen, V., Sidorenko, D., Wolf-Gladrow, D. A., & Völker, C. (2014). A skill assessment of the biogeochemical model REcoM2 coupled to the finite element sea ice ocean model (FESOM 1.3). *Geoscientific Model Development*, *7*(6), 2769–2802. https://doi.org/10.5194/gmd-7-2769-2014

Siemer, J. P., Machín, F., González-Vega, A., Arrieta, J. M., Gutiérrez-Guerra, M. A., Pérez-Hernández, M. D., et al. (2021). Recent trends in SST, Chl-a, productivity and wind stress in upwelling and open ocean areas in the upper eastern North Atlantic subtropical gyre. *Journal of Geophysical Research: Oceans*, *126*(8), e2021JC017268. https://doi.org/10.1029/2021JC017268

Solomon, S., Plattner, G.-K., Knutti, R., & Friedlingstein, P. (2009). Irreversible climate change due to carbon dioxide emissions. *Proceedings of the National Academy of Sciences*, *106*(6), 1704–1709. https://doi.org/10.1073/pnas.0812721106

Sydeman, W. J., García-Reyes, M., Schoeman, D. S., Rykaczewski, R. R., Thompson, S. A., Black, B. A., & Bograd, S. J. (2014). Climate change and wind intensification in coastal upwelling ecosystems. *Science*, *345*(6192), 77–80. https://doi.org/10.1126/science.1251635

Terhaar, J., Goris, N., Müller, J. D., DeVries, T., Gruber, N., Hauck, J., et al. (2023). Assessment of global ocean biogeochemistry models for ocean carbon sink estimates in reccap2 and recommendations for future studies. *ESS Open Archive*. https://doi.org/10.22541/essoar.168394734.41886821/v1

Tsujino, H., Urakawa, L. S., Griffies, S. M., Danabasoglu, G., Adcroft, A. J., Amaral, A. E., et al. (2020). Evaluation of global ocean–sea-ice model simulations based on the experimental protocols of the Ocean Model Intercomparison Project phase 2 (OMIP-2). *Geoscientific Model Development*, *13*(8), 3643–3708. https://doi.org/10.5194/gmd-13-3643-2020

Tsujino, H., Urakawa, S., Nakano, H., Small, R. J., Kim, W. M., Yeager, S. G., et al. (2018). JRA-55 based surface dataset for driving ocean–sea-ice models (JRA55-do). *Ocean Modelling*, *130*, 79–139. https://doi.org/10.1016/j.ocemod.2018.07.002

Varela, R., Álvarez, I., Santos, F., de Castro, M., & Gómez-Gesteira, M. (2015). Has upwelling strengthened along worldwide coasts over 1982-2010? *Scientific Reports*, *5*(1), 10016. https://doi.org/10.1038/srep10016

Virtanen, P., Gommers, R., Burovski, E., Oliphant, T. E., Weckesser, W., Cournapeau, D., et al. (2020). Scipy/scipy: Scipy 1.6.0 [Software]. *Zenodo*. https://doi.org/10.5281/zenodo.4406806

Virtanen, P., Gommers, R., Oliphant, T. E., Haberland, M., Reddy, T., Cournapeau, D., et al. (2020). SciPy 1.0 contributors (2020). SciPy 1.0: Fundamental algorithms for scientific computing in Python. *Nature Methods*, *17*(3), 261–272. https://doi.org/10.1038/s41592-019-0686-2

Wang, Q., Danilov, S., Sidorenko, D., Timmermann, R., Wekerle, C., Wang, X., et al. (2014). The Finite Element Sea Ice-Ocean model (FESOM) v.1.4: Formulation of an ocean general circulation model. *Geoscientific Model Development*, *7*(2), 663–693. https://doi.org/10.5194/gmd-7-663-2014

Yasunaka, S., Manizza, M., Terhaar, J., Olsen, A., Yamaguchi, R., Landschützer, P., et al. (2023). An assessment of CO_2 uptake in the arctic ocean from 1985 to 2018. *Global Biogeochemical Cycles*, *37*(11), e2023GB007806. https://doi.org/10.1029/2023GB007806

References From the Supporting Information

Aumont, O., Ethé, C., Tagliabue, A., Bopp, L., & Gehlen, M. (2015). PISCES-v2: An ocean biogeochemical model for carbon and ecosystem studies. *Geoscientific Model Development*, *8*(8), 2465–2513. https://doi.org/10.5194/gmd-8-2465-2015

Berthet, S., Séférian, R., Bricaud, C., Chevallier, M., Voldoire, A., & Ethé, C. (2019). Evaluation of an online grid-coarsening algorithm in a global eddy-admitting ocean biogeochemical model. *Journal of Advances in Modeling Earth Systems*, *11*(6), 1759–1783. https://doi.org/10.1029/2019MS001644

Gürses, O., Oziel, L., Karakuş, O., Sidorenko, D., Völker, C., Ye, Y., et al. (2023). Ocean biogeochemistry in the coupled ocean–sea ice–biogeochemistry model FESOM2.1–REcoM3. *Geoscientific Model Development*, *16*(16), 4883–4936. https://doi.org/10.5194/gmd-16-4883-2023

Lacroix, F., Ilyina, T., Mathis, M., Laruelle, G. G., & Regnier, P. (2021). Historical increases in land-derived nutrient inputs may alleviate effects of a changing physical climate on the oceanic carbon cycle. *Global Change Biology*, *27*(21), 5491–5513. https://doi.org/10.1111/gcb.15822

Law, R. M., Ziehn, T., Matear, R. J., Lenton, A., Chamberlain, M. A., Stevens, L. E., et al. (2017). The carbon cycle in the Australian community climate and Earth system simulator (ACCESS-ESM1)—Part 1: Model description and pre-industrial simulation. *Geoscientific Model Development*, *10*(7), 2567–2590. https://doi.org/10.5194/gmd-10-2567-2017

Nakano, H., Tsujino, H., Hirabara, M., Yasuda, T., Motoi, T., Ishii, M., & Yamanaka, G. (2011). Uptake mechanism of anthropogenic CO_2 in the Kuroshio extension region in an ocean general circulation model. *Journal of Oceanography*, *67*(6), 765–783. https://doi.org/10.1007/s10872-011-0075-7

Orr, J., & Epitalon, J. (2015). Improved routines to model the ocean carbonate system: Mocsy 2.0. *Geoscientific Model Development*, *8*(3), 485–499. https://doi.org/10.5194/gmd-8-485-2015

Orr, J. C., Najjar, R. G., Aumont, O., Bopp, L., Bullister, J. L., Danabasoglu, G., et al. (2017). Biogeochemical protocols and diagnostics for the CMIP6 Ocean Model Intercomparison Project (OMIP). *Geoscientific Model Development*, *10*(6), 2169–2199. https://doi.org/10.5194/gmd-10-2169-2017

Séférian, R., Nabat, P., Michou, M., Saint-Martin, D., Voldoire, A., Colin, J., et al. (2019). Evaluation of CNRM Earth system model, CNRM-ESM2-1: Role of Earth system processes in present-day and future climate. *Journal of Advances in Modelling Earth Systems*, *11*(12), 4182–4227. https://doi.org/10.1029/2019MS001791

Sakamoto, K., Nakano, H., Urakawa, S., Toyoda, T., Kawakami, Y., Tsujino, H., & Yamanaka, G. (2023). Reference manual for the meteorological research institute community Ocean Model version 5 (MRI.COMv5) (Tech. Rep. No. 87). *Meteorological Research Institute*. https://doi.org/10.11483/mritechrepo.87

Sarmiento, J. L., & Gruber, N. (2006). Carbon cycle. In *Ocean biogeochemical dynamics* (pp. 318–358). Princeton University Press.

Schwinger, J., Goris, N., Tjiputra, J. F., Kriest, I., Bentsen, M., Bethke, I., et al. (2016). Evaluation of NorESM-OC (versions 1 and 1.2), the ocean carbon-cycle stand-alone configuration of the Norwegian Earth System Model (NorESM1). *Geoscientific Model Development*, *9*(8), 2589–2622. https://doi.org/10.5194/gmd-9-2589-2016

Urakawa, L. S., Tsujino, H., Nakano, H., Sakamoto, K., Yamanaka, G., & Toyoda, T. (2020). The sensitivity of a depth-coordinate model to diapycnal mixing induced by practical implementations of the isopycnal tracer diffusion scheme. *Ocean Modelling*, *154*, 101693. https://doi.org/10.1016/j.ocemod.2020.101693

Wanninkhof, R., Park, G.-H., Takahashi, T., Sweeney, C., Feely, R., Nojiri, Y., et al. (2013). Global Ocean carbon uptake: Magnitude, variability and trends. *Biogeosciences*, *10*(3), 1983–2000. https://doi.org/10.5194/bg-10-1983-2013

Wright, R. M., Le Quéré, C., Buitenhuis, E., Pitois, S., & Gibbons, M. J. (2021). Role of jellyfish in the plankton ecosystem revealed using a global ocean biogeochemical model. *Biogeosciences*, *18*(4), 1291–1320. https://doi.org/10.5194/bg-18-1291-2021